Results in Physics 7 (2017) 3349–3352

Contents lists available at ScienceDirect

Results in Physics

journal homepage: www.journals.elsevier.com/results-in-physics

Influence of the oxygen partial pressure on the growth and optical properties of RF-sputtered anatase TiO_2 thin films

A.R. Grayeli Korpi [a], Sahare Rezaee [b], C. Luna [c], Ş. Ţălu [d], A. Arman [e,*], A. Ahmadpourian [f]

[a] Physics and Accelerators Research School, Nuclear Sciences and Technology Research Institute, Tehran, Iran
[b] Department of Physics, Kermanshah Branch, Islamic Azad University, Kermanshah, Iran
[c] Universidad Autónoma de Nuevo León, Facultad de Ciencias Físico Matemáticas, Av. Universidad s/n, San Nicolás de los Garza 66455, Nuevo León, Mexico
[d] Technical University of Cluj-Napoca, Faculty of Mechanical Engineering, Department of AET, Discipline of Descriptive Geometry and Engineering Graphics, 103-105B-dulMuncii St., Cluj-Napoca 400641, Cluj, Romania
[e] Young Researchers and Elite Club, Kermanshah Branch, Islamic Azad University, Kermanshah, Iran
[f] Young Researchers and Elite Club, Arak Branch, Islamic Azad University, Arak, Iran

ARTICLE INFO

Article history:
Received 5 July 2017
Received in revised form 26 July 2017
Accepted 7 August 2017
Available online 11 August 2017

Keywords:
TiO_2 films
RF reactive magnetron sputtering
XRD
AFM
Swanepoel method

ABSTRACT

Titanium dioxide (TiO_2) films with thicknesses around 300 nm were deposited on glass substrates by reactive radio frequency (RF) magnetron sputtering at constant RF sputtering power (200 W), high sputtering pressure and room temperature. The effects of the oxygen presence on the growth and properties of the films were investigated using mixtures of Ar and O_2 with different $O_2/(Ar + O_2)$ ratios (from 0.0 to 0.3) during the sample deposition. The crystalline properties and surface morphology were characterized using X-ray diffraction (XRD) and atomic force microscopy (AFM), respectively. The optical properties were studied by ultraviolet–visible–near infrared (UV–Vis–NIR) spectroscopy, and the refractive index and the thickness of the samples were obtained using the Swanepoel method. The obtained results indicate that all the TiO_2 films grew with an anatase phase and with an improved crystallinity at $O_2/(Ar + O_2) = 0.2$. However, AFM studies show that the grain size and surface roughness decrease as the $O_2/(Ar + O_2)$ ratio increases from 0.0 to 0.3. Moreover, a maximum refractive index was obtained for the sample prepared at $O_2/(Ar + O_2) = 0.2$.

Introduction

The versatile properties of titanium dioxide (TiO_2) have been intensively studied for several decades [1] with an increasing interest for its numerous potential applications [2]. Specifically, its electronic, mechanical, catalytic, hydrophilic/hydrophobic and optical properties have attracted huge interest for their exploitation in photocatalysis [2,3], solar cells [4], water splitting [5], self-cleaning and antifogging surfaces [6], heat mirrors [7], disinfection of surfaces, water and air [8,9], pigments [10], sunscreens and cosmetics [11], implants [12] and cancer treatment [13], among others.

In many of these applications the titanium dioxide-based materials are required in the form of nanoparticles, one-dimensional (1D) nanomaterials or thin films. Therefore, with one or more of their dimensions reduced to the nanoscale, such materials play the role of tiny active units in miniaturized devices, or coating layers that enhance the functionality of another materials [2,3]. In fact, the highly transparent and anti-reflection properties of Titania thin films become these materials excellent optical coating layers [6], which are crucial for optical systems and solar cell technologies [7]. On the other hand, the properties of these low dimensional materials are strongly dependent on the size of their nanoscopic dimensions, their morphology, surface roughness, presence of doping agents, contact with other semiconductor materials and crystalline microstructure; thus, these properties can be engineered according to the used preparation method and the synthesis conditions [14].

At atmospheric pressure, TiO_2 can grow with three crystalline phases: rutile (tetragonal), anatase (tetragonal) and brookite (orthorhombic). While rutile is the more thermodynamically stable phase of TiO_2 at all pressures and temperatures, anatase is frequently the first phase formed in many synthesis routes because this phase requires a less constrained structural re-arrangement to grow from an amorphous precursor, and displays a lower surface energy in comparison with the rutile phase [15–17].

* Corresponding author.
E-mail address: ali.arman173@gmail.com (A. Arman).

http://dx.doi.org/10.1016/j.rinp.2017.08.018
2211-3797/

Table 1
Grain size (D), average surface roughness (R_{ave}) rms surface roughness and thickness calculated with the Sanepoel method of samples produced at various $O_2/Ar + O_2$ ratios.

Sample	$O_2/Ar + O_2$ ratio	D (nm)	R_{ave} (nm)	R_{rms} (nm)	Thickness (nm)
1	0	144.2	18.9	17.2	304.12
2	0.1	121.5	14.2	11.6	299.51
3	0.2	26.0	3.4	3.6	295.94
4	0.3	18.1	2.0	2.6	295.06

Different methods have been used to prepare titanium dioxide films such as radio frequency sputtering [18–20], pulse laser deposition [21,22] and sol-gel methods [23,24], obtaining films with properties dependent on the preparation techniques and the deposition conditions [25–31].

In the present investigation, the influence of the $O_2/(Ar + O_2)$ ratio in the deposition of TiO_2 thin films by magnetron sputtering, and the possible correlations between the structural and optical properties of TiO_2 thin films have been studied.

Experimental details

Titanium dioxide thin films were deposited on glass substrates via reactive radio frequency (RF) magnetron sputtering system [32–34] using a pure TiO_2 target (purity 99.99%) with a diameter of 76.2 mm. The glass substrates ($20 \times 20 \times 1$ mm^3) were ultrasonically cleaned in acetone and ethanol. The base pressure of the deposition chamber was kept at 5×10^{-6} Torr, and all depositions were carried out under a constant working pressure of 5×10^{-3} Torr and a RF power of 200 W. The deposition rate was measured by a quartz crystal deposition rate controller (Sigma Instruments, SQM-160, USA) positioned close to the substrate. Four samples were deposited using mixtures of Ar (purity 99.999%) and O_2 (purity 99.999%) with $O_2/(Ar + O_2)$ ratios of 0.0, 0.1, 0.2 or 0.3, respectively.

The crystalline phases present in the samples were identified by X-ray diffraction (XRD) using a STOE Stadi MP diffractometer and CuKα radiation (λ = 1.54056 Å). The XRD were collected with step size of 0.01° and a scan rate of 1.0 s per step. The film surface morphology and roughness were analyzed with an atomic force microscope (AFM, NT-MDT scanning probe microscope, model BL022). The root mean square roughness (R_{rms}) and average grain diameter were determined analyzing AFM images over a 4 μm^2 image area and using Nova software and JMicroVision Code. Several samples were used in all analysis to guarantee reproducibility of the results. The details of samples produced in the present investigation are given in Table 1.

Optical transmittance of the films was recorded at room temperature using an ultraviolet–visible–near-infrared (UV–VIS–NIR) spectrometer (Hitachi model U-3501), and the Swanepoel method [35] was used to calculate the film thickness and optical constants such as refractive index. Specifically, the film thickness was calculated from the interference fringes found in the optical transmittance spectra using the following equation [36]:

$$d = \frac{\lambda_1 \lambda_2}{2(\lambda_1 n_2 - \lambda_2 n_1)} \quad (1)$$

where n_1 and n_2 are the refractive indices at two adjacent transmittance maxima at λ_1 and λ_2, respectively. The refraction number, N, was calculated from the transmittance maxima, T_M, and transmittance minima, T_m, of the interference fringes observed in the UV–VIS–NIR spectra of the TiO_2 thin films on glass substrates using the equation:

$$N = 2s\frac{T_M - T_m}{T_M T_m} + \frac{s^2 + 1}{2} \quad (2)$$

where s is the substrate refractive index.

The refractive index, n, of the films was then calculated according to the following equation [35]:

$$n = \left[N + (N^2 - s^2)^{\frac{1}{2}}\right]^{\frac{1}{2}} \quad (3)$$

Results and discussion

XRD results

Fig. 1 shows the XRD patterns of TiO_2 films deposited at room temperature and different $O_2/(Ar + O_2)$ ratios. These patterns show three well-defined diffraction peaks at 2θ values corresponding to the planes (1 0 1), (2 0 0) and (2 1 1) of the anatase crystalline phase (JCPDS 21-1272). Samples display a polycrystalline nature in agreement with the observations of other works using sputter deposition techniques [37], and in contrast with the preferred orientation found in TiO_2 films deposited by dip coating, spin coating and screen printing techniques [6]. From Fig. 1 it is observed that the intensity of the anatase peaks depends on the oxygen concentration used during sample preparation, increasing the peak intensities as the $O_2/(Ar + O_2)$ ratio is increased from 0 to 0.2, and decreasing again for $O_2/(Ar + O_2) = 0.3$. It seems that an excessive presence of oxygen during TiO_2 thin film deposition hinders the crystallization of the anatase phase.

AFM results

Fig. 2 depicts the AFM images of the four samples prepared at different $O_2/(Ar + O_2)$ ratios, and Table 1 shows the grain size, layer thickness, average roughness (R_{ave}) and root mean square roughness (R_{rms}) obtained from the AFM analysis of all samples. The decrease of physical grain size with the O_2 addition is obvious in Fig. 2. In addition, the surface roughness results indicate that an increasing $O_2/(Ar + O_2)$ ratio from 0.0 to 0.3 during the growth of the samples leads to smoother surfaces, reducing the surface roughness from 18.9 nm to 2.0 nm, respectively. The roughness of the films is an important factor that affects physical behaviors of TiO_2 thin films, especially optical properties. Therefore, the large

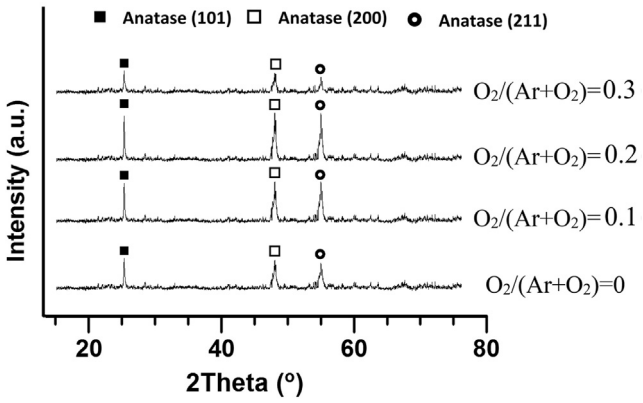

Fig. 1. XRD patterns of various samples produced at different $O_2/Ar + O_2$ ratios.

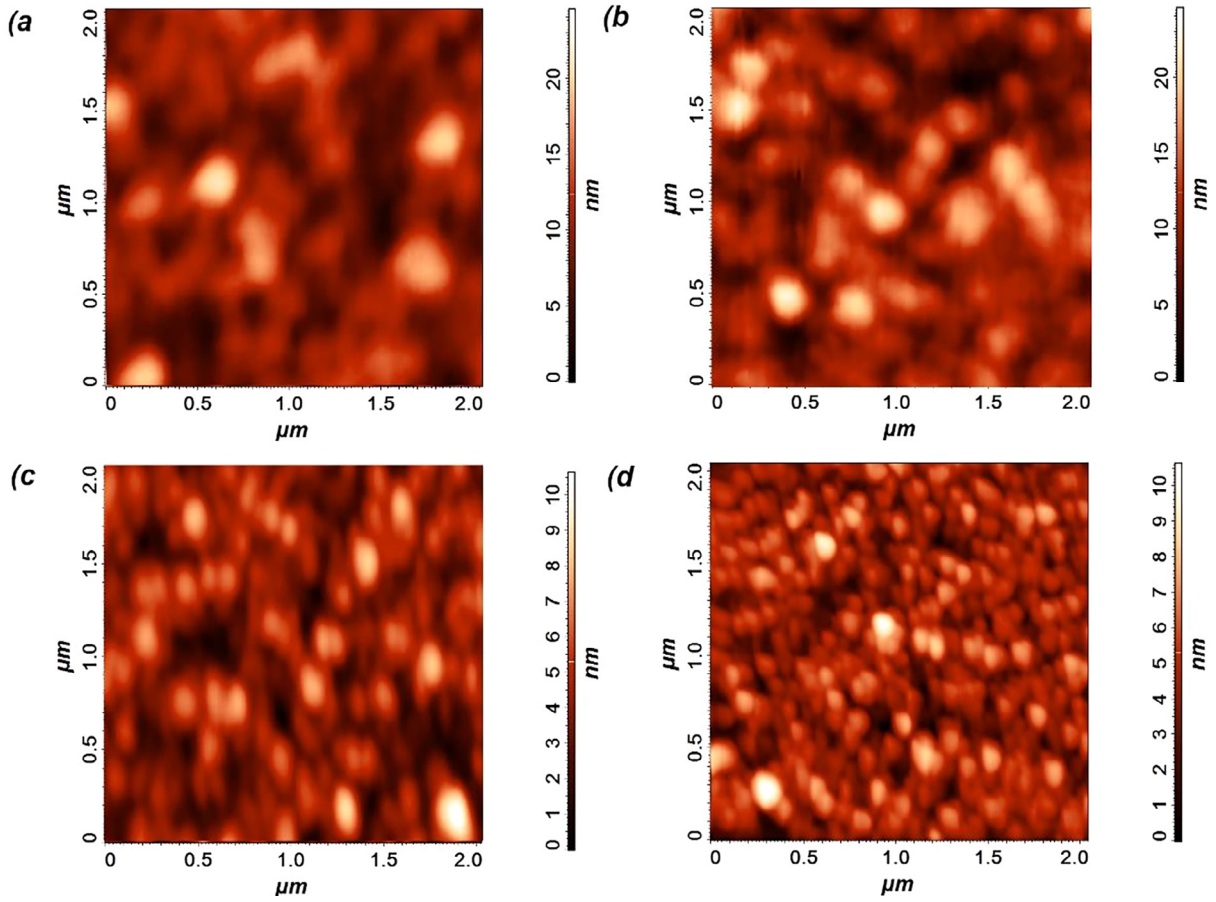

Fig. 2. AFM images of various samples produced at different $O_2/Ar + O_2$ ratios: a) 0 b) 0.1 c) 0.2 d) 0.3.

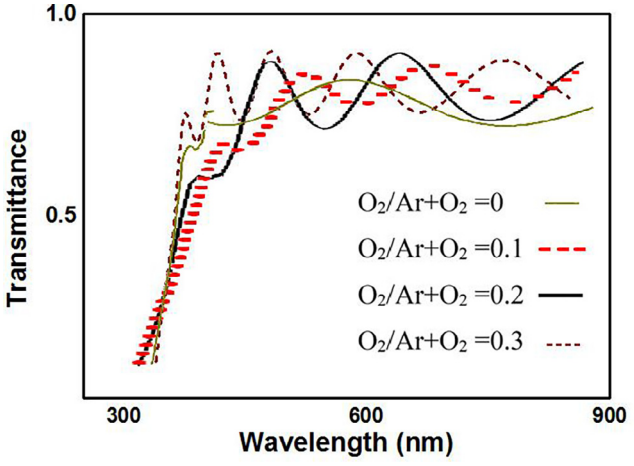

Fig. 3. Optical transmittance spectra of various samples produced at different $O_2/Ar + O_2$ ratios.

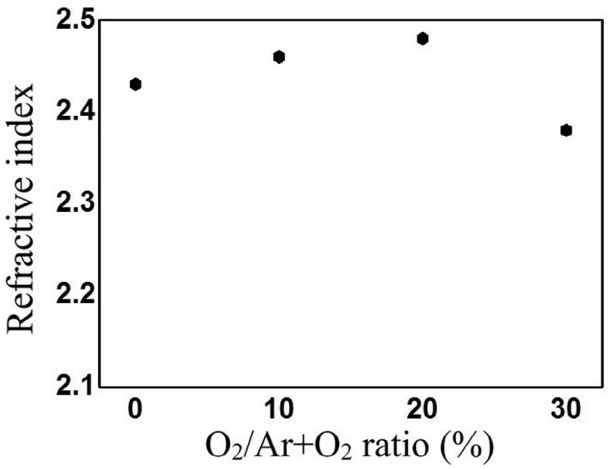

Fig. 4. Variation in the refractive index as a function of $O_2/Ar + O_2$ ratios.

roughness of the thin film grown in pure Ar ambient should contribute significantly to the optical loss of this sample. Thus, it can be concluded that a small amount of oxygen added during sputtering deposition is desirable to obtain TiO_2 films with improved optical characteristics.

Optical results

Fig. 3 shows the transmittance spectra of the TiO_2 films grown on the substrates at various $O_2/(Ar + O_2)$ ratios and at the constant power (200 W). Transmittance and the number of oscillations in the transmittance spectra increased with increasing O_2 concentration (Fig. 3).

The average transmittance of the different samples is about 85% in the visible region with respect to reference blank glass substrate. The sample prepared at pure Ar ambient shows a decrease in visible light transmittance, probably due to its larger surface roughness.

The refractive index and film thickness of samples were evaluated using Swanepoel method. The calculated film thickness of all

samples is close to 300 nm (Table 1), which is in good agreement with the monitored thickness during the deposition experiment.

The variation in the refractive index calculated from Swanepoel method is plotted as a function of the $O_2/(Ar + O_2)$ ratio in Fig. 4. It is found that the refractive index of samples prepared with $O_2/(Ar + O_2)$ ratios of 0.0, 0.1, 0.2 and 0.3 are 2.43, 2.46, 2.48 and 2.38, respectively. This trend shows that the refractive index initially increases with the increment of the O_2 addition up to $O_2/(Ar + O_2) = 0.2$, and then, it decreases for the sample deposited at $O_2/(Ar + O_2) = 0.3$. The observed increase may be attributed to higher packing density and a change in the sample crystallinity. This behavior of the refractive index implies that a small amount of O_2 concentration reduces the film damage and, as a result, enhances the packing density of the film, while larger O_2 concentrations can causes a reduction of the packing density.

Conclusion

Anatase TiO_2 thin films have been deposited on glass substrates by RF magnetron sputtering using mixtures of Ar and O_2 with $O_2/(Ar + O_2)$ ratios from 0.0 to 0.3. We found that the crystallinity and surface roughness of these films are noticeably dependent on the presence of small oxygen concentrations during the preparation of samples, and the competence of their effects determine the optical properties of the final films. In this way, the grain size of the films and the surface roughness significantly decrease as the O_2 addition is increased, however, the crystallinity of the films is improved at relative oxygen concentrations of $O_2/(Ar + O_2) = 0.2$. Also, the refractive index exhibit a maximum value for the sample prepared with $O_2/(Ar + O_2) = 0.2$.

References

[1] Renz C. Helv Chim Acta 1921;4:961–8.
[2] Fujishima A, Rao TN, Tryk DA. J Photochem Photobiol C: Photochem Rev 2000;1:1–21.
[3] Pichat P. An overview of the potential applications of TiO_2 photocatalysis for food packaging, medical implants, and chemical compound delivery. Photocatalysis 2016:345–67.
[4] Nazeeruddin MK, Humphry-Baker R, Liska P, Grätzel M. J Phys Chem B 2003;107:8981–7.
[5] Sheridan MV, Hill DJ, Sherman BD, Wang D, Marquard SL, et al. Nano Lett 2017;17:2440–6.
[6] Euvananont C, Junin C, Inpor K, Limthongkul P, Thanachayanont C. Ceram Int 2008;34:1067–71.
[7] Okada M, Tazawa M, Jin P, Yamada Y, Yoshimura K. Vacuum 2006;80:732–5.
[8] Huang Z, Maness PC, Blake DM, Wolfrum EJ, Smolinski SL, Jacoby WA. J Photochem Photobiol A: Chem 2000;130:163–70.
[9] Foster HA, Ditta IB, Varghese S, Steele A. Appl Microbiol Biotechnol 2011;90:1847–68.
[10] Bardet R, Belgacem MN, Bras J. Cellulose 2013;20:3025–37.
[11] Tucci P, Porta G, Agostini M, et al. Cell Death Dis 2013;4:e549.
[12] Hazan R., Sreekantan S., Mydin R.B.S., Abdullah Y., Mat I., Study of TiO2 nanotubes as an implant application. In: A.A. Mohamed, F.M. Idris, A.B. Hasan, Z. Hamzah (Eds.), AIP Conference Proceedings, vol. 1704(1), 040009. AIP Publishing.
[13] Sakai H, Ito E, Cai R, Yoshioka T, Kubota Y, Hashimoto K, Fujishima A. Biochim Biophys Acta 1994;1201:259.
[14] Daghrir R, Drogui P, Robert D. Ind Eng Chem Res 2013;52:3581–99.
[15] Sharma AK, Thareja RK, Willer U, Schade W. Appl Surf Sci 2003;206:137–48.
[16] Shin H, Jung HS, Hong KS, Lee JK. J. Sol. St. Chem. 2005;178:15–21.
[17] Zhang H, Banfield JF. J Mater Chem 1998;8:2073–6.
[18] Huang CH, Tsao CC, Hsu CY. Ceram Int 2011;37:2781–8.
[19] Sima C, Waldhauser W, Lackner J, Kahn M, Nicolae I, Viespe C, Grigoriu C, Manea A. J Opt Adv Mater 2007;9:1446–9.
[20] Nair PB, Justinvictor VB, Daniel GP, Joy K, Raju KC, Kumar DD, Thomas PV. Prog Nat Sci Mater Int 2014;24(3):218–25.
[21] Farkas B, Budai J, Kabalci I, Heszler P, Geretovszky Z. Appl Surf Sci 2008;254:3484–90.
[22] Nechachea R, Nicklaus M, Diffalah N, Ruediger A, Rosei F. Appl Surf Sci 2014;313:48–52.
[23] Parna R, Joost U, Nommiste E, Kaambre T, Kikas A, Kuusik I, Irsimaki MH, Kink I, Kisand V. Appl Surf Sci 2011;257:6897–901.
[24] Dastan D, Londhe PU, Chaure NB. J Mater Sci: Mater Electron 2014;25 (8):3473–9.
[25] Kubo Y, Iwabuchi Y, Yoshikawa M, Sato Y, Shigesato Y. J Vac Sci Technol, A 2008;26(4):893–7.
[26] Yang C, Fan H, Xi Y, Chen J, Li Z. Appl Surf Sci 2008;254:2685–9.
[27] Malagutti A, Moura H, Garbin J, Ribeiro C. Appl Catal B 2009;90:205–12.
[28] Kollbek K, Sikora M, Kapusta C, Szlachetko J, Zakrzewska K, Kowalski K, Radecka M. Appl Surf Sci 2013;281:100–11.
[29] Dastan D, Panahi SL, Chaure NB. J Mater Sci: Mater Electron 2016;27 (12):12291–6. http://dx.doi.org/10.1007/s10854-016-4985-4.
[30] Manohari A, Dhanapandian S, Kumar K, Mahalingam T. Int J Thin Film Sci Technol 2014;3:1–6.
[31] Dastan D, Leila Panahi S, Yengntiwar AP, Banpurkar AG. Adv Sci Lett 2016;22 (4):950–3.
[32] Molamohammadi M, Arman A, Achour A, Astinchap B, Ahmadpourian A, Boochani A, Naderi S, Ahmadpourian A. J Mater Sci: Mater Electron 2015;26:5964–9.
[33] Ahmadpourian A, Luna C, Boochani A, Arman A, Achour A, Rezaee S, Naderi S. Eur Phys J Plus 2016;131:381.
[34] Arman A, Ţălu Ş, Luna C, Ahmadpourian A, Naseri M, Molamohammadi M. J Mater Sci: Mater Electron 2016;26:9630–9.
[35] Swanepoel R. J Phys E: Sci Instrum 1983;16:1214–21.
[36] Hong WQ. J Phys D Appl Phys 1989;22:1384–90.
[37] Hasan MM, Haseeb ASMA, Saidur R, Masjuki HH, Hamdi M. Opt Mater 2010;32:690–5.